THE JOURNAL OF PHYSICAL CHEMISTRY A

 VOLUME 108, NUMBER 1, JANUARY 8, 2004

ARTICLES

Surface-Induced Dissociation of Polyatomic Hydrocarbon Projectile Ions with Different Initial Internal Energy Content

A. Qayyum,[†,||] Z. Herman,[†,‡] T. Tepnual,[†] C. Mair,[†] S. Matt-Leubner,[†] P. Scheier,[†] and T. D. Märk*[,†,§]

Institut für Ionenphysik, Leopold-Franzens Universität, Technikerstr. 25, A-6020 Innsbruck, Austria, V. Čermák Laboratory, J. Heyrovský Institute of Physical Chemistry, Academy of Sciences of the Czech Republic, Dolejškova 3, 182 23 Prague 8, Czech Republic, and Department of Plasma Physics, Comenius University, Mlynska dolina, SK-842 48 Bratislava, Slovak Republic

Received: June 12, 2003; In Final Form: October 8, 2003

The specific effect of initial internal energy of CH_5^+, $C_2H_4^+$, $C_2H_5^+$, and $C_2H_6^+$ ions on the extent of surface-induced fragmentation was investigated. The ions were prepared either in a gas discharge Colutron type (using a hydrogen-methane mixture at 0.2−0.5 Torr) or in a low-pressure Nier-type electron impact ion source using various target gases. Whereas projectile ions from the Colutron source are thermalized due to collisions in the high pressure environment and thus contained a negligible amount of internal energy, projectile ions from the Nier-type ion source resulting from direct electron impact ionization reactions have internal energies up to several eV. Their internal energy content was estimated using break-down curves and photoelectron spectra from literature. Results obtained here show that their different initial internal energy content had a considerable effect on the extent of fragmentation of the surface-excited projectile ions: ions with initial internal energy fragmented at much lower collision energies than internally relaxed projectile ions. It appears that the initial internal energy content of the projectile ions is entirely preserved in the projectile ion during the ion/surface collision, and thus is available in the subsequent dissociative processes as additional energy to the internal energy acquired by the projectile ion in the surface-excitation process.

l. Introduction

Surface-induced dissociation (SID) of polyatomic ions has received considerable attention in recent years. On one hand, surface-induced dissociation has been investigated as an alternative method to gas-phase collision-induced dissociation (CID) to characterize organic ions by their fragmentation pathways in the mass spectrometric analysis.[1−5] Alternatively, ion-surface collisions have been used to characterize the nature of surfaces, to modify their properties, and to investigate chemical reactions at surfaces.[1−5] In addition to fundamental importance, interactions of molecular ions, especially small hydrocarbon ions, are relevant to technological applications such as plasma−wall interactions in electrical discharges and fusion plasmas.[6−8] Hydrocarbon molecules are also emitted in large quantities into the Earth's atmosphere, and some of them may be ionized in the upper layers of the atmosphere and react with surfaces of aerosols.[9] An analogous situation occurs in the interstellar medium, where interactions of ions with surfaces of dust are of importance.

Understanding polyatomic ion−surface interactions requires, among others, a detailed knowledge of energy transfer in ion−

* Corresponding author; E-mail: tilmann.maerk@uibk.ac.at.
[†] Leopold-Franzens Universität.
[‡] Academy of Sciences of the Czech Republic.
[§] Comenius University.
[||] Permanent address: Pakistan Institute of Nuclear Science and Technology, P. O. Nilore, Islamabad, Pakistan.

10.1021/jp030747m CCC: $27.50
Published on Web 12/11/2003

surface collisions. The overall energy balance in an ion−surface collision is

$$E_{TOT} = E_{tr} + E_{int} = E'_{int} + E'_{tr} + E'_{surf} \quad (1)$$

where E_{tr} is the translational energy of the incident projectile, E_{int} is the initial internal excitation energy of the projectile, E'_{int} is the internal energy of the surface-excited projectile ion after the collision, E'_{tr} is the translational energy of the product ions, and E'_{surf} is the fraction of energy absorbed by the surface. Over the past fifteen years, several terms in eq 1 were investigated to specify their effect on the fragmentation of a polyatomic projectile. The influence of the translational energy of the projectiles on the fragmentation process was obtained from studies of collision energy resolved mass spectra (CERMS), and CERMS curves have been obtained for a large number of projectiles.[1−5,10−12] The fraction of collisional energy transformed in a surface collision into the internal energy of the projectile ion was also subject of several studies for a variety of projectiles and for a number of different surfaces.[1,5,13−19] Moreover, information on the translational energy of the product ions and their angular distributions have been obtained from ion−surface scattering experiments.[14−16] Finally, the fraction of total energy absorbed by the surface has been calculated from theoretical models or determined experimentally either directly[20] or from the overall balance of eq 1.[14−16] The least addressed problem so far appears to be the role of the initial internal energy of the polyatomic projectile, E_{int}, in the surface-excited projectile ion fragmentation.

The surface collision of a polyatomic ion has been characterized as a multimode excitation process in which energy is exchanged between surface modes and polyatomic projectile ion modes. The question is how efficient is this energy exchange. The internal energy of a polyatomic projectile ion has been usually kept as low as possible in the experiments in which energy partitioning according to eq 1 was investigated[14−16] in order to allow an easier overall balancing of the different terms in eq 1. Thus, the question remains what is the role of a possible initial internal energy content in the projectile ion in surface reaction processes such as surface-induced dissociation (SID). For instance, is the initial energy content fully randomized between the surface modes and internal modes of the projectile ion, or is it at least partly retained within the projectile ion and thus influences the subsequent dissociation processes after the surface collision?

The effect of initial internal energy of the projectile ion on surface-induced dissociation was examined in a careful study of C_{60}^+ fragmentation on HOPG.[18] The projectile ions were prepared either by laser desorption/ionization (LDI) or by evaporation and ionization by 7.9 eV VUV laser radiation. In the former case, the average internal energy content of C_{60}^+ was estimated to about 27.4−31.4 eV, while in the latter case it was below 0.3 eV. The surface-induced fragmentation of the "hot" C_{60}^+ prepared by LDI was indeed larger than the fragmentation of the "colder", oven-evaporated and single-photon ionized C_{60}^+. Quantification of this effect by fitting the experimental spectra with simulated spectra based on RRKM calculations led to a difference in average energy content of about 12 eV and to the conclusion that a significant fraction (at least 50%) of the internal energy is retained during the surface collision and contributes toward fragmentation of the surface-scattered C_{60}^+. These findings were consistent with the results of the effect of vibrational excitation on surface-induced dissociation of NO^+ on GaAs(110).[21] The incident vibrational energy was found to be as much as 10 times more effective than translational energy in forming the O^+ dissociation product.

To address this question, we carried out here a series of experiments on surface dissociation of several simple polyatomic hydrocarbon ion projectiles, prepared with different internal energy contents (see also a recent short report[22] on similar results for the simple ions CH_3^+ and CH_4^+). In particular, we investigated the influence of their initial internal energy on the surface-induced decomposition of the projectile ion by measuring (secondary) mass spectra of the product ions as a function of the collision energy in the low energy range of about 0 to 80 eV.

2. Experimental Section

Experiments were carried out with the tandem mass spectrometer apparatus BESTOF described in detail in our earlier papers.[4,10] It consists of a double focusing two-sector-field mass spectrometer (reversed geometry) combined with a linear time-of-flight mass spectrometer. Projectile ions were produced either in a low-pressure Nier-type electron impact ion source or at elevated pressures in a Colutron gas discharge source. The ions produced were extracted from the ion source region and accelerated to 3 keV for mass (and energy) analysis by a double-focusing two-sector-field mass spectrometer. After passing the mass spectrometer exit slit, the ions were refocused by an Einzel lens and decelerated to the required collision energy by a system of deceleration lenses before interacting with the target surface. Shielding the target area with conical shield plates minimized field penetration effects. The incident impact angle of the projectile ions was kept at 45°, and the scattering angle (defined as a deflection from the incident beam direction) was fixed at 91°.

The collision energy of ions impacting on the surface is defined by the potential difference between the ion source and the surface. The potential difference (hence, the collision energy) can be varied from about zero to about 2 keV with a typical resolution of about 200 meV (full width at half-maximum in the case of the Nier-type ion source and of about 1 eV in the case of the Colutron-type ion source). The collision energy and a measure of the projectile beam energy spread was obtained by applying to the target a retarding potential and measuring the (reflected) total ion signal as a function of the target potential.

A fraction of the product ions formed at the surface exited the shielded chamber through a 1 mm diameter orifice. The ions were then subjected to a pulsed extraction-and-acceleration field that initiated the time-of-flight analysis of the ions. The second mass analyzer was a linear time-of-flight mass selector with a flight tube of about 80 cm length. The mass selected ions were detected by a double-stage multichannelplate, connected to a multichannel scaler (time resolution of 5 ns per channel) and a laboratory computer. The product ion intensities to be used in the CERMS plots were obtained by integration of the recorded mass spectral ion signals; this removed instrumental effects such as those due to the minima present in the center of the measured product ion mass peaks and the different widths of the peaks for different masses (see mass spectra in Figure 1).

The Nier-type source was a commercial CH5 mass spectrometer source[23] operated at pressures of about 10^{-5} Torr and at temperatures of 100 to 200 C. Ions were prepared by interaction of 120 eV electrons with ethylene (producing the projectile ion $C_2H_4^+$), ethane (yielding $C_2H_4^+$, $C_2H_5^+$, $C_2H_6^+$), or propane ($C_2H_5^+$). The projectile ion CH_5^+ was produced in

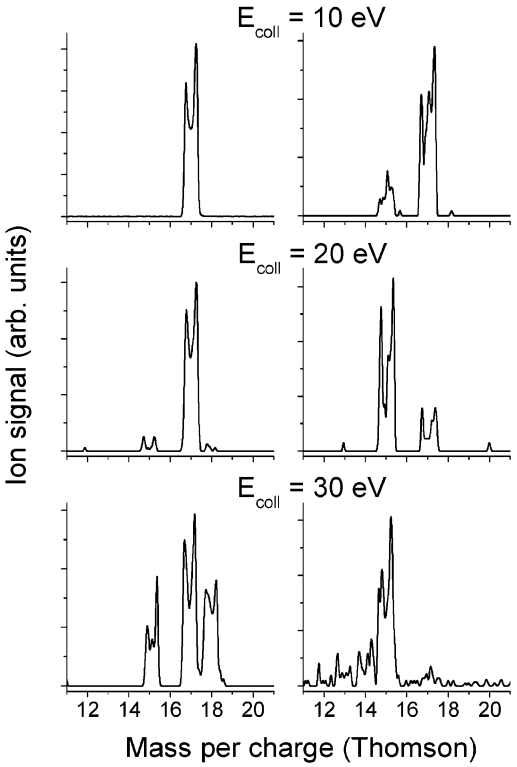

Figure 1. Mass spectra of product ions from collisions of CH_5^+ with a hydrocarbon-covered stainless steel surface at collision energies of 10, 20, 30. Spectra on the left side: CH_5^+ from the Colutron source. Spectra on the right side: CH_5^+ from the Nier-type source. In the Colutron source data, at 30 eV, the signal at *m*/*z* 18 is evidently H_2O^+, presumably from H-atom transfer surface reaction of a small amount of impurity OH^+ ions in the CH_5^+ beam.

the same source via ion−molecule reactions $CH_4^+ + CH_4 \rightarrow CH_3 + CH_5^+$ by using a methane target gas and increasing the ion source pressure to about 5×10^{-4} Torr. The Colutron source was operated with a 9:1 hydrogen/methane mixture at a pressure of 0.2−0.5 Torr. The main process is evidently ionization of hydrogen and subsequent charge transfer between hydrogen ions and methane; a variety of hydrocarbon ions including C_1, C_2, and C_3 group ions are then formed by successive ion−molecule reactions.

The surface used here was a polished stainless steel surface maintained under ultrahigh vacuum conditions (10^{-9} Torr) in a bakeable turbo-pump evacuated target collision chamber. However, even these conditions did not exclude deposition of multilayers of hydrocarbon contaminants on the surface, whenever the valve between the mass spectrometer and the target collision chamber was opened and the pressure in the target region increased to the 10^{-8} Torr range. The surface was thus a hydrocarbon-covered metal surface as in our earlier studies, thereby mimicking a "real" surface as occurring in many situations dealing with plasma−wall interactions in low and high pressure and low and high-temperature plasmas.[6−8]

3. Results

3.1. Collision Energy Resolved Mass Spectra (CERMS). This section summarizes data obtained for the projectile ions CH_5^+, $C_2H_4^+$, $C_2H_5^+$, and $C_2H_6^+$. We will first present the data by plotting the relative abundance of the product ions as a function of collision energy of the particular projectile ions in the form of CERMS plots. For most of the projectile ions we have measured data by producing the respective projectile ion in the Nier-type and in the Colutron type ion source. A

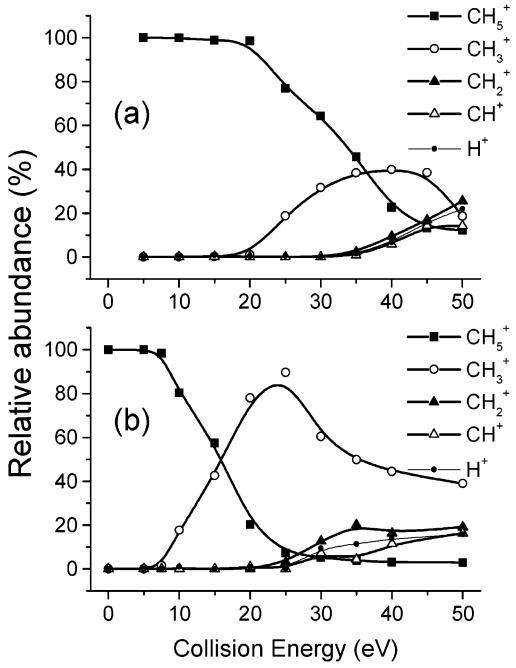

Figure 2. Collision energy resolved mass spectra (CERMS curves) for CH_5^+ projectile ions. (a) CH_5^+ from the Colutron source. (b) CH_5^+ from the Nier-type source.

corresponding discussion concerning a quantification of the internal energy content of these projectile ions produced in the two different ion sources will be given in section 3.2, followed by a discussion of the CERMS in light of this information in section 3.3.

CH_5^+. Figure 1 shows product ion mass spectra obtained at collision energies of 10, 20, and 30 eV for the projectile ion CH_5^+ produced in the Colutron- and the Nier-type ion source, respectively. In addition to the fragment ions CH_3^+, CH_2^+, and CH^+, the reaction products $C_2H_3^+$ and $C_2H_5^+$ were observed in both cases in the collision energy range up to 50 eV. The latter two C_2-group ions were shown earlier[16,22,24−26] using the same surface and deuterated molecular projectile ions to result partly from surface chemical sputtering reactions and partly by chemical reactions of the projectile ion with terminal CH_3-groups of surface hydrocarbons. Surface-induced chemical reactions (SIR) and surface sputtering are not the subject of this paper and will not be discussed further (for more details see refs 16, 22, 24−26). Figure 2 summarizes the SID data for CH_5^+ surface-induced dissociations in the form of CERMS curves. Surface-induced dissociation leads to product ions CH_3^+, CH_2^+, and CH^+; however, for the projectile ion from the Colutron source the thresholds are shifted to higher collision energies by about 5−15 eV. As will be demonstrated in detail below, the ions from the Nier type ion source have a considerably higher internal energy content than those from the Colutron source, and it is this difference in internal energy content which manifests itself dramatically in the extent of the projectile ion fragmentation at the same collision energy.

$C_2H_4^+$. The CERMS curves for the $C_2H_4^+$ projectile ion extracted from the Colutron source and from the Nier-type source (produced by electron impact ionization of either ethylene or ethane) are shown in Figure 3a−c, respectively. The product ions of surface-induced dissociation processes are in all cases $C_2H_3^+$ and $C_2H_2^+$. The product ion $C_2H_5^+$ results evidently from a hydrogen pick-up reaction, when the reactive radical cation $C_2H_4^+$ collides with the hydrocarbon-covered metal surface. A fraction of the product ion $C_2H_3^+$ and the product ion CH_3^+

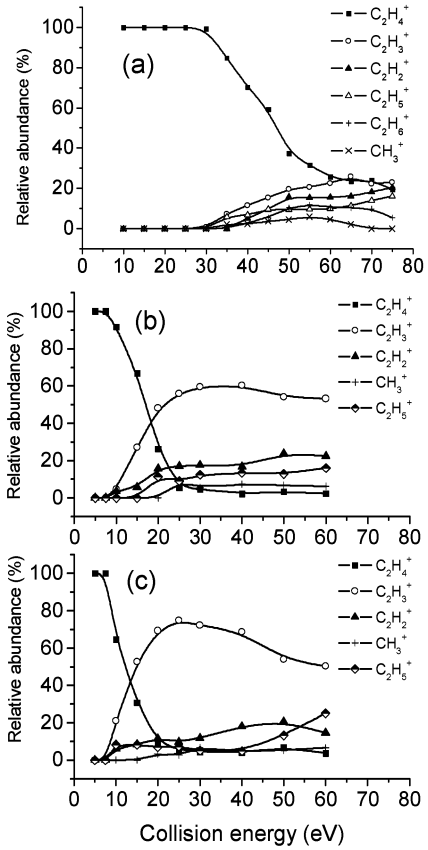

Figure 3. Collision energy resolved mass spectra (CERMS curves) for $C_2H_4^+$ projectile ions. (a) $C_2H_4^+$ from the Colutron source. (b) $C_2H_4^+$ from the Nier-type source by electron impact ionization of ethylene. (c) $C_2H_4^+$ from the Nier-type source by electron impact ionization of ethane.

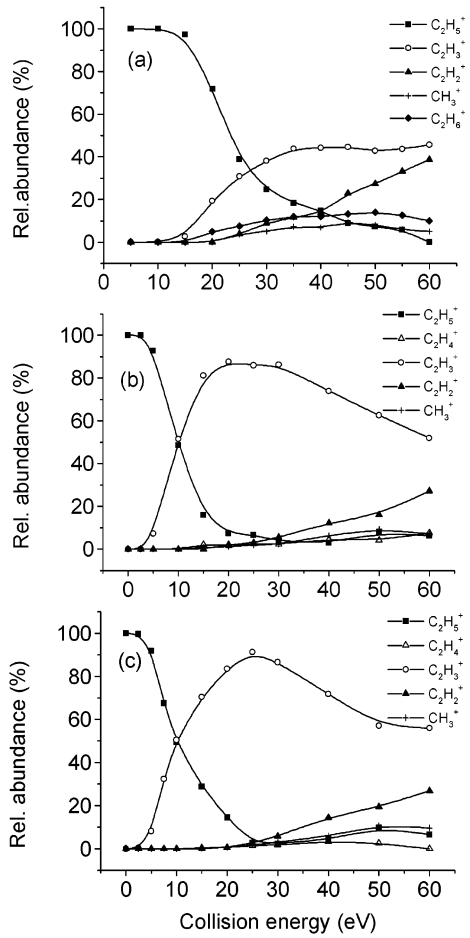

Figure 4. Collision energy resolved mass spectra (CERMS curves) for $C_2H_5^+$ projectile ions. (a) $C_2H_5^+$ from the Colutron source. (b) $C_2H_5^+$ from the Nier-type source by electron impact ionization of ethane. (c) $C_2H_5^+$ from the Nier-type source by electron impact ionization of propane.

are presumably dissociation products of this chemical reaction product ion $C_2H_5^+$. For the Colutron-produced $C_2H_4^+$, most of the secondary ions appear at collision energy of about 30−35 eV, while for ions from the Nier-type source the dissociative and the reactive channels set in at considerably lower collision energies. Again, the lower onsets of fragmentation thresholds for projectile ions produced by electron impact in the Nier-type source suggest a higher internal energy content of these projectile ions in comparison with $C_2H_4^+$ formed in the Colutron source. An increased amount of $C_2H_3^+$ in the CERMS curves of $C_2H_4^+$ from the Nier-type source may indicate a more efficient surface reaction yielding $C_2H_5^+$ (which subsequently fragments to $C_2H_3^+ + H_2$) than in the case of ions produced in the Colutron ion source.

$C_2H_5^+$. Figure 4a−c summarizes the CERMS curves obtained with the projectile ion $C_2H_5^+$ produced either in the Colutron source at rather high hydrogen/methane mixture pressures (a), or produced by electron impact in the low-pressure Nier-type source either from ethane (b) or propane (c). Higher onsets of dissociative processes and a considerably higher relative amount of the main dissociation product $C_2H_3^+$ with the Colutron-produced $C_2H_5^+$ in comparison with $C_2H_5^+$ from the Nier-type source again indicate a higher internal energy content of the latter projectile ions.

$C_2H_6^+$. These projectile ions could be produced only by electron impact ionization from ethane in the Nier-type source, and thus no comparison with Colutron-produced projectile ions is possible. The product ions formed by surface-induced fragmentation are $C_2H_5^+$, $C_2H_4^+$, $C_2H_3^+$, $C_2H_2^+$, and CH_3^+.

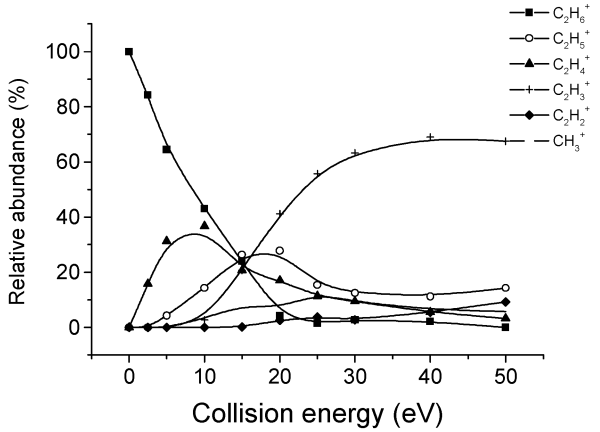

Figure 5. Collision energy resolved mass spectra (CERMS curves) for $C_2H_6^+$ projectile ions produced in the Nier-type source by electron impact ionization of ethane.

They are thus the same ion species as produced by fragmentation of the ethane molecular ion after electron or photon impact.[27,28] Indeed, the CERMS curves in Figure 5 resemble somewhat the break-down pattern of the ethane molecular ion, as known from coincidence photoelectron spectroscopy studies[27] and from theoretical calculations,[29] however, they are considerably smeared out by a rather broad distribution of translational-to-internal energy transferred in the surface collision (for more information on this subject see refs 14−18, 30, 31 and references therein).

In general, this confirms earlier suggestions that, due to the character of the translational-to-internal energy transfer in the ion−surface collisions, the CERMS curves contain information on the break-down patterns of the projectiles.[12,17,30]

3.2. Internal Energy of the Projectile Ions. The CERMS curves shown in the previous section clearly indicated that there is a difference in the extent of projectile ion fragmentation between the projectile ions formed in the hydrogen/methane mixture in the Colutron ion source at pressures of 0.2−0.5 Torr and the same projectile ions formed by electron impact in the low pressure ($\sim 10^{-5}-10^{-4}$ Torr) Nier-type ion source. This different fragmentation behavior must be related to different properties, and one obvious property in which these two categories of projectile ions differ is their internal energy content. The two components that determine the internal energy content of the projectile ions are the internal energy acquired in the surface collision from the translational-to-internal energy transfer from the translational energy of the projectile ion and the initial internal energy of the projectile ion from the initial preparation process (ionization, chemical reaction etc.). In the following, an attempt will be made to estimate quantitatively this initial internal energy from general information available on the two different production routes.

For the ions formed in the low-pressure Nier-type source by electron impact ionization, the projectile ions originate from ionization of the neutral molecule or from possible subsequent unimolecular dissociation of the excited molecular ion. Therefore, their internal energy content can be estimated from the break-down pattern of the respective molecular ion and the photoelectron spectrum of the particular molecule. The break-down pattern specifies the range of excitation energies of the molecular ion, over which a particular ion is stable, and the photoelectron spectrum indicates the probability of deposition of a certain excitation energy into the molecular ion during the Franck−Condon-governed ionization process. It is assumed in this estimation that the impact of electrons of energies above 70 eV leads to the same energy deposition as photon impact, i.e., autoionization processes are neglected. The internal energy distribution of a nonfragmenting molecular ion, $P(E_{int})$, is then given by

$$P(E_{int})_M = I_{NM}(E_{int})\, W_{ph}(E_{exc}) \qquad (2)$$

where $I_{NM}(E)$ is the normalized intensity of the molecular ion in the break-down pattern at the internal energy E_{int}, $W_{ph}(E_{exc})$ is the probability of depositing E_{exc} in the molecular ion as given by the photoelectron spectrum, and $E_{exc} = E_{ph} - IE$ (E_{ph} photon energy, IE is the ionization energy of a molecule). For fragment ions an analogous equation holds

$$P(E_{int})_F = I_{NF}(E'_{int})\, W_{ph}(E'_{exc}) \qquad (3)$$

except that $E'_{exc} = A(E_{ph} - AE)$, where AE is the appearance energy of the fragment ion. We assume that at this threshold the entire excitation energy of the molecular ion is used to drive the dissociation process and the fragment ion is formed practically without excitation energy. At higher energies, the original excitation energy of the molecular ion is statistically distributed over the internal degrees of freedom of the ion and only a certain part of it ends as internal energy of the fragment ion, the rest going into the excitation energy of the neutral fragment and into the degrees of freedom of relative motion of the two fragments formed. This is taken into account by a factor A which expands the internal energy scale of the fragment ion by $1/A = (3N_M - 6)/(3N_F - 6)$, where N_M and N_F is the number of atoms in the molecular and fragment ion, respectively.

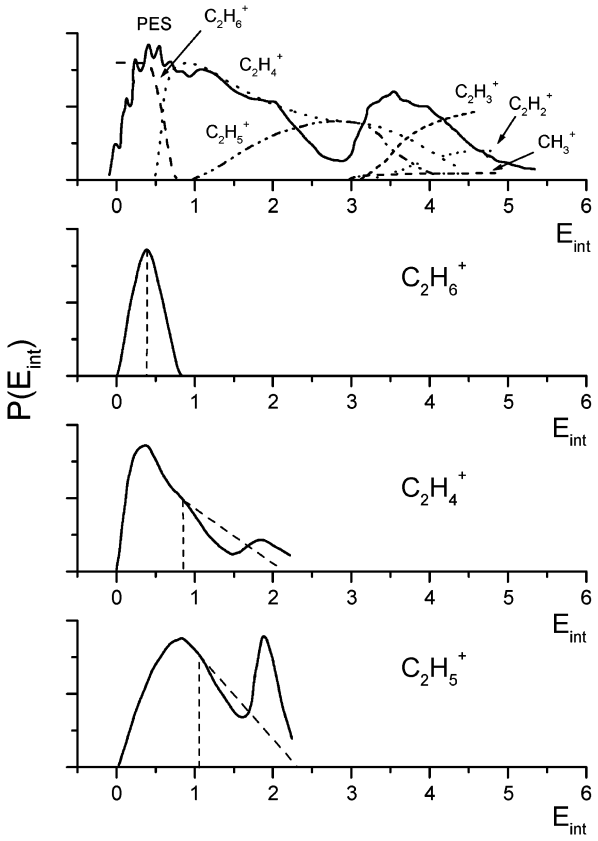

Figure 6. Estimation of the internal energy distribution of the projectile ions $C_2H_6^+$, $C_2H_4^+$, and $C_2H_5^+$, produced by electron impact ionization of ethane in the Nier-type source. Upper part: photoelectron spectrum of ethane (PES) and break-down curves of the ethane molecular ion. Below: estimated $P(E_{int})$ of the molecular ion $C_2H_6^+$ and of the fragment ions $C_2H_4^+$ and $C_2H_5^+$, respectively. Vertical dashed lines mean value of E_{int}. Dashed parts of curves mean extrapolated simplified form of $P(E_{int})$.

In Figure 6 we show the internal energy for $C_2H_6^+$, $C_2H_5^+$, and $C_2H_4^+$ formed by electron impact ionization of ethane using these considerations. The figure gives in the top panel the break-down pattern of the molecular ethane ion[27] and the photoelectron spectrum of ethane[31,32] and in the lower three panels the $P(E_{int})$ derived for the projectile ions $C_2H_6^+$, $C_2H_5^+$, and $C_2H_4^+$. It becomes immediately apparent that these ions formed by electron impact in the low-pressure Nier-type source (see Figure 6) contain an appreciable amount of internal energy. For instance, the average internal energy, $(E_{int})_{av}$ for $C_2H_6^+$ is about 0.4 eV and it extends up to 0.8 eV, $(E_{int})_{av}$ for $C_2H_5^+$ is about 0.8 eV and it extends up to 2.2 eV, and $(E_{int})_{av}$ for $C_2H_4^+$ is about 1.1 eV and it extends up to 2.4 eV.

Analogously, for the molecular ion $C_2H_4^+$, formed by electron impact on ethylene, the initial internal energy distribution was estimated from the break-down pattern of this molecular ion[33] and the photoelectron spectra[32,34] (Figure 7). It is characterized by two groups of internal energies $(E_{int})_{av}$ $(C_2H_4^+) = 0.25$ eV and $\langle 0;1.0\rangle$, and $(E_{int})_{av}$ $(C_2H_4^+) = 2.4$ eV and $\langle 2.0;2.8\rangle$. Finally, for the fragment ion $C_2H_5^+$ from propane, the value $(E_{int})_{av}$-$(C_2H_5^+) = 1.1$ eV and $\langle 0;2.5\rangle$ was obtained from the break-down pattern of the propane molecular ion[35] and the photoelectron spectrum of propane.[32] For the projectile ion CH_5^+ formed in the electron impact ionization source at relatively high gas pressures via a slightly exoergic (0.16 eV) ion molecule reaction between CH_4^+ and a methane molecule, one can only

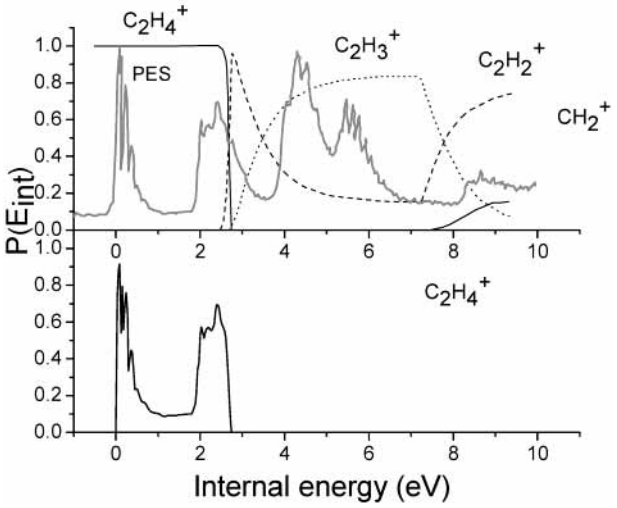

Figure 7. Same as Figure 6 but for $C_2H_4^+$.

roughly estimate that the internal energy content will be not much different from that of the reactant ion CH_4^+ (originally produced by electron impact of methane, see ref 22), i.e., $(E_{int})_{av}$-$(CH_5^+) \sim 1.0$ eV.

Estimation of the internal energy of projectile ions formed in the Colutron source is more difficult. In the 9:1 hydrogen/methane mixture used here at pressures of 0.2−0.5 Torr, the main process will be most likely ionization of hydrogen by electron impact and charge transfer between hydrogen ions and methane. The hydrogen molecular ion H_2^+ is known to exhibit three different recombination energies:[36] (a) 16.4−17.4 (from H_2^+ with v′∼4 and small internuclear distances R to H_2); (b) 13−14 eV (from H_2^+ with v′∼4 and large R to H_2); (c) about 11 eV (from H_2^+ with v′∼4 and large R to $H_2(^3\Sigma^+_u)$). The recombination energies (c) (not sufficient to ionize methane) and (a) (allowing effective dissociative ionization of methane) should not contribute to CH_4^+ formation. A more detailed treatment of charge-transfer transitions between various vibrational levels of H_2^+ suggests that via recombination energy (b) the projectile ion is presumably formed close to the ionization potential with maximally a few tenths of eV of internal energy. The ion can react further to CH_5^+, and in the mixture other hydrocarbon ions can be formed by successive chemical reactions. However, these ions can relax their internal energy in nonreactive collisions with surplus hydrogen and methane, and thus a plausible conclusion is that most of the projectile ions from the Colutron source are considerably relaxed ions, i.e., with internal energy close to zero.

3.3. Ion Survival Probability. A large fraction of projectile ions is neutralized in the surface collision. The ion survival probability, S_a, for CH_5^+ was estimated earlier[16] for impact on a hydrogen-covered carbon (HOPG − highly oriented pyrolytic graphite) under an incident angle of 30° with respect to the surface to be 12−18% in the incident energy range 15−50 eV. Ion survival probability for $C_2H_4^+$ and $C_2H_5^+$ has been determined in our recent experiments[37] to be about the same. All these data refer to projectile ions with initial internal energy as estimated above. It can be expected that the properties of hydrocarbon-covered stainless steel will be similar to the hydrocarbon-covered carbon, i.e., determined primarily by the adsorbed hydrocarbon layer. However, the ion survival probability depends strongly on the incident angle, decreasing with increasing angle from the surface. The dependence was measured by us earlier for open-shell and closed-shell polyatomic ions striking a hydrocarbon-covered stainless steel surface.[14] When increasing the incident angle from 30° to 45°, the relative survival probability of the projectile ions decreased about 6 times. Therefore, one may roughly estimate that in the experiments described here the survival probability of the projectile ions CH_5^+, $C_2H_4^+$, and $C_2H_5^+$ for the incident angle of 45° was about 2−3% in the incident energy range 15−50 eV.

4. Discussion

The CERMS curves given in section 3.1 clearly show that there is a substantial difference in the extent of fragmentation between the projectiles prepared either in a Colutron source or by electron impact ionization in a low-pressure Nier-type source. Projectile ions from the Colutron source, prepared in a 9:1 hydrogen/methane mixture at fairly high pressures of 0.2−05 Torr, appear to be largely relaxed by collisions in the source and cause a considerably smaller extent of fragmentation than the ions from the Nier-type source. The projectile ions prepared by electron-impact ionization in the Nier-type source have internal energies of a few tenths up to more than 1 eV, and the corresponding energy distribution has been estimated in section 3.2. The presence of this initial internal energy is evidently the reason for the larger extent (at lower energies) of fragmentation of these projectile ions. Therefore, qualitatively one can conclude that the internal energy of the projectile ion is not equilibrated with the surface in the surface collision and remains conserved to a considerable extent (see below) in the surface excited projectile and contributes to its subsequent fragmentation.

In the following, an attempt will be made to estimate the effect of the internal energy to the SID process quantitatively for each of the ions studied with both ion sources. For instance, the observed appearance thresholds for fragment ions in the collision energy dependence should, in principle, correspond to those ions containing the maximum possible initial internal energy, i.e., in the case of ions from the Colutron, the necessary dissociation energy at the threshold will be supplied only by translational energy transferred into internal energy during the surface collision, whereas in the case of ions from the Nier source, additional energy will be available due to the initial internal energy. Thus, values for these appearance energies and shifts in these values may be used to characterize possible internal energy differences, and this method has been already successfully applied for the simple hydrocarbon ions CH_3^+ and CH_4^+ in ref 22.

Alternatively, one can also use the energy position of similar fragmentation features in the different (Colutron- versus Nier-type ion source) CERMS curves to characterize possible internal energy differences. Such features are, for instance, characteristic crossings between CERMS curves, i.e., the crossing of the decreasing projectile ion curve with an increasing product ion curve. These crossing points indicate that the same degree of dissociation has been reached, however, by different amounts of initial internal energies and different amounts of internal energy transferred during the collision. In the following, the energy differences in the thresholds or in the position of the characteristic crossings will be used to estimate the effect of the initial internal energy content of a specific projectile ion on the SID process.

CH_5^+. The difference in threshold values (linear extrapolation of the data) for the fragment ions produced in SID of CH_5^+ projectile ions from the Colutron source (Figure 2a) and from the Nier-type source (2b) is as follows: $(15.8 - 6.7) = 9.1$ eV for CH_3^+, $(33.8 - 21.1) = 12.7$ eV for CH_2^+, and $(34.8 - 23.2) = 11.6$ eV for CH^+. The average value of the translational-

to-internal energy transfer on hydrocarbon-covered metal or carbon surfaces has been well established[12,14−19,30] as being about 6% of the collision energy with an effective width of about ±1.5 eV. Using this energy transfer efficiency it is possible to calculate from these measured differences in the thresholds the corresponding difference in internal energy of 0.6, 0.8, and 0.7 eV, respectively. This value is in fair agreement with the average initial internal energy roughly estimated for CH_5^+ formed in the chemical reaction of CH_4^+ in the Nier-type source, ∼1.0 eV.

Alternatively, one can use the crossing points of the CERMS curves $CH_5^+-CH_3^+$, $CH_5^+-CH_2^+$, $CH_5^+-CH^+$ for the projectile ions CH_5^+ produced in the two different ways (Figure 2). The differences are (35−17) = 18 eV, (45−27) = 17 eV, and (45−29) = 16 eV for the above-mentioned crossings, respectively. With the above-mentioned 6% efficiency of translational-to-internal energy transfer, one arrives at values of 1.1, 1.0, and 0.9 eV, respectively. Although these data are less reliable (the curve for CH_5^+ from the Colutron source may be shifted to somewhat higher values due to a certain admixture of background OH^+), the values for internal energy from threshold data and from curve-crossing data are mutually consistent and in fair agreement with the estimation of the internal energy content of CH_5^+ from reactions in the Nier-type source (about 1 eV). Therefore, these results are consistent with the hypothesis that the projectile ion CH_5^+ from the Colutron source has only a very small internal energy, while that one from the Nier-type source has a rather large internal energy, and this energy is fully used as additional energy to drive the SID reaction, thereby leading to the observed downward shift in crossing points when going from the Colutron results to the Nier results.

$C_2H_4^+$. For this projectile ion we can also observe a huge shift in the CERMS crossing points, i.e., the crossing point between the $C_2H_4^+$ and $C_2H_3^+$ curve shifts as shown in Figure 3 from 64 eV (in the case of the Colutron) to 18 eV ($C_2H_4^+$ from ethylene in the Nier source) and to 14 eV ($C_2H_4^+$ from ethane in the Nier source). This implies a change in the internal energy of 2.8 and 3.0 eV, respectively. These values are larger than the average values of the internal energy content of the two ions from the Nier-type source derived in section 3.2. However, it should be noted that part of the $C_2H_3^+$ ions result from a surface chemical reaction chain (see above: H-atom transfer reaction to $C_2H_4^+$ leads to $C_2H_5^+$ which further decomposes to $C_2H_3^+$)) and thus the $C_2H_3^+$ signal in particular from the Nier source is increased by $C_2H_3^+$ from the chemical reaction, yielding an additional shift in crossing points. A strong indication that this may be the case is the relatively much larger abundance of the $C_2H_3^+$ ion in the two lower panels of Figure 3. Nevertheless, this shift and the much lower threshold values for all of the product ions (when going from the Colutron results to the Nier results) indicate again that the ions from the Nier-type source have a considerable internal energy content.

For the $C_2H_4^+$ projectile ion, appearance energies and respective shifts can be employed too to obtain corresponding information about internal energy content and energy transfer. For instance, it is clearly visible that the threshold for the appearance of the $C_2H_3^+$ ion and for the $C_2H_2^+$ are shifted when going from Figure 3a to 3b downward from a value of about 30 eV to 35 eV (Figure 3a) to about 7.5 eV (Figure 3c; we do not discuss here the example given in Figure 3b as in this case two different ion distributions are contributing in the case of the Nier source and thus it will be difficult to interpret the results in detail). Using the energy transfer efficiency of 0.06 it is possible to calculate from these measured differences in the threshold values the corresponding difference in internal energy between ions produced in the Colutron and the Nier source, yielding a value of about 1.5 eV (i.e., 25 × 0.06 = 1.5 eV). Because we are dealing with threshold data, this difference should be caused by the maximum difference in the internal energy of the two projectiles. The maximum internal energy excitation of the $C_2H_4^+$ from electron impact ionization in the Nier-type source was estimated to lie at about 2 eV and, assuming no internal energy for the ions from the Colutron source, there is semiquantitative agreement with the above derived difference of 1.5 eV in particular when taking into account that the effective width of the energy transferred by the surface collision may be up to 1.5 eV fwhm.

Thermochemical thresholds for dissociation processes of $C_2H_4^+$ to $C_2H_3^+$+ H and $C_2H_2^+ + H_2$ can be derived from literature data[38,39] to lie between 2.6 and 2.7 eV with no clear indication which of the ions has the lower threshold (the relatively inaccurate data in Figure 7 indicate $C_2H_2^+$ to have the lower threshold with a value of about 2.3 eV). The present results indicate in the case where no initial internal energy is involved (i.e., see the data in Figure 3a for the Colutron source) that both fragment ions appear at a threshold value of about 30 to 35 eV. Using the energy transfer efficiency of 0.06 it is possible to calculate from this an absolute value for the thermochemical threshold yielding a value of approximately 1.8 to 2.1 eV. This value is close to the values discussed above (2.3 up to 2.7) in particular taking into account that the effective width of this energy transferred is 1.5 eV.

In conclusion, the data are again consistent with the assumption that the Colutron-produced $C_2H_4^+$ is practically completely relaxed as far as its internal energy is concerned, while the Nier-type source $C_2H_4^+$ ions contain substantial amounts of internal energy that is fully effective as additional energy to the internal energy acquired in the surface excitation in the subsequent dissociation processes.

$C_2H_5^+$. The shift between the crossing point between the CERMS curves for $C_2H_5^+$ and $C_2H_3^+$ (see Figure 4) when going from $C_2H_5^+$ prepared in the Colutron source to $C_2H_5^+$ from the Nier-type source (ions produced from both ethane and propane) is (27 − 9) = 19 eV. This implies a change in the translational-to-internal energy conversion of 1.08 eV (again, for the efficiency of 0.06 E_{tr}). The average internal energy content of $C_2H_5^+$ ion from both ethane and propane was estimated as $(E_{int})_{av}(C_2H_5^+)$ = 1.1 eV, in very good agreement with the observed shift in the CERMS curve crossings. Therefore, we can conclude that in the case of ions from the Colutron, the $C_2H_5^+$ projectile ions have no appreciable amount of internal energy and thus the entire energy defect must be supplied by the internal energy acquired in the surface collision, whereas in the case of ions from the Nier-type source the $C_2H_5^+$ projectile ions have an average internal energy of 1.1 eV which is fully used to complement the energy acquired in the surface collision to enable the dissociation to take place.

Because of the fact that the threshold values for the appearance of the various fragment ions lie already for the ions from the Colutron source at rather low collision energies, it is not possible to deduce here meaningful information about the internal energy and its use for SID from the appearance energies and their shifts in the case of the Nier-type ion source.

$C_2H_6^+$. The data available refer only to $C_2H_6^+$ from the Nier-type source. Because there are no data for projectiles produced with different internal energies, no discussion of its effect may be given.

All of the above-reported data on dissociative processes in collisions of simple hydrocarbon ions, formed in two different ways, with hydrocarbon-covered stainless steel surface show quite clearly, that there is a difference in the extent of fragmentation of the projectile ion − as reflected in the CERMS curves − for ions formed in the high-pressure Colutron source and in the low-pressure Nier-type source. The difference is due to the fact that the ions produced in the Colutron source have low or negligible internal energies, whereas ions formed by electron impact ionization in the low-pressure Nier-type source contain some excitation energy, which can be estimated using the information from break-down curves and photoelectron spectra of the systems in question. The differences in thresholds of various dissociation processes and in crossing points of the CERMS curves of the product ions indicate that the internal energy of the projectile ions is practically entirely preserved in the projectile during the surface collision and it can be fully used in the subsequent dissociative processes as an additional energy to the internal energy acquired by the ion in the surface-excitation process.

As has been shown earlier,[22] in a polyatomic ion−surface collision, a part of the collision energy is transformed into the internal energy of the projectile in a process that can be described as a multimode excitation. Vice versa, one might in principle expect that the internal excitation of the projectile could flow during the surface collision into the surface and cause at least a partial de-excitation of the projectile ion. This does not seem to be the case. A possible way of explaining this phenomenon is that the initial internal energy of the projectile is distributed over all internal degrees of freedom of the incoming projectile ion and thus cannot be effectively transferred into the surface, while the surface-excitation process, occurring during a short-duration collision, leads to excitation of only some modes of the projectile. The energy of the projectile acquired in the surface collision is subsequently redistributed over the internal degrees of freedom to be then used, together with the initial internal excitation of the projectile, in the unimolecular dissociation process.

Acknowledgment. This work has been carried out within the Association EURATOM-ÖAW in cooperation with the Association EURATOM-IPP.CR. The content of the publication is the sole responsibility of the authors and does not necessarily represent the views of the EU Commission or its services. Partial support of this work by FWF, ÖNB and ÖAW Wien, Austria, by the European Community, Brussels, and by the Grant Agency of the Czech Republic (Grant No. 203/00/632, is gratefully acknowledged.

References and Notes

(1) Cooks, R. G.; Ast, T.; Mabud, M. D. A. *Int. J. Mass Spectrom.* **1990**, *100*, 209.

(2) *Polyatomic-Surface Interactions, Int. J. Mass Spectrom.*; Hanley, L., Ed. **1998**, 174.

(3) Wörgötter, R.; Mair, C.; Fiegele, T.; Grill, V.; Märk, T. D.; Schwarz, H. *Int. J. Mass Spectrom. Ion Proc.* **1997**, *164*, L1.

(4) Mair, C.; Fiegele, T.; Biasioli, F.; Wörgötter, R.; Grill, V.; Lezius, M.; Märk, T. D. *Plasma Sources Sci. Technol.* **1999**, *8*, 191.

(5) Grill, V.; Shen, J.; Evans, C.; Cooks, R. G. *Rev. Sci. Instrum.* **2001**, *72*, 3149.

(6) Hofer, W. O.; Roth, J. *Physical Processes of the Interaction of Fusion Plasmas with Solids*; Academic Press: San Diego, 1996.

(7) *Atomic and Molecular Processes in Fusion Edge Plasma*; Janev, R. K., Ed., Plenum: New York, 1995.

(8) *Atomic and molecular data and their application*; Mohr, P. J., Wiese, W. L., Eds.; AIP Conference proceedings 434, American Institute of Physics: Woodbury, New York, 1998.

(9) Hewitt, C. N. *Reactive Hydrocarbons in the atmosphere;* Academic Press: San Diego, 1999.

(10) Mair, C.; Fiegele, T.; Biasioli, F.; Herman, Z.; Märk, T. D. *J. Chem. Phys.* **1999**, *111*, 2770.

(11) Mair, C.; Herman, Z.; Fedor, J.; Lezius, M.; Märk, T. D. *J. Chem. Phys.* **2003**, *118*, 1479.

(12) Mair, C.; Lezius, M.; Herman, Z.; Märk, T. D. *J. Chem. Phys.* **2003**, *118*, 7090.

(13) Wysocki, V. H.; Kenttämaa, H. I.; Cooks, R. G. *Int. J. Mass Spectrom., Ion Proc.* **1987**, *75*, 181.

(14) Kubišta, J.; Dolejšek, Z.; Herman, Z. *Eur. Mass Spectrom.* **1998**, *4*, 311.

(15) Žabka, J.; Dolejšek, Z.; Roithová, J.; Grill, V.; Märk, T. D.; Herman, Z. *Int. J. Mass Spectrom.* **2001**, *213*, 145.

(16) Roithová, J.; Žabka, J.; Dolejšek, Z.; Herman, Z. *J. Phys. Chem. B* **2002**, *106*, 8293.

(17) Mair, C., Ph.D. Thesis, Universität Innsbruck, Austria, 2001.

(18) Beck, R. D.; Rockenberger, J.; Weiss, P.; Kappes, M. *J. Chem. Phys.* **1996**, *104*, 3638.

(19) Biasioli, F.; Fiegele, T.; Mair, C.; Herman, Z.; Echt, O.; Aumayr, F.; Winter, H.; Märk, T. D. *J. Chem. Phys.* **2000**, *113*, 5053.

(20) Aschyultz, D. G.; Wainhaus, S. B.; Hanley, L.; Claire, P. D. S.; Hase, W. L. *J. Chem. Phys.* **1997**, *106*, 10337.

(21) Martin, J. S.; Greeley, J. N.; Morris, J. R.; Feranchak, B. T.; Jacobs, D. C. *J. Chem. Phys.* **1994**, *100*, 6791.

(22) Qayyum, A.; Tepnual, T.; Mair, C.; Matt-Leubner, S.; Scheier, P.; Herman, Z.; Märk, T. D. *Chem. Phys. Lett.* **2003**, *376*, 539.

(23) Matt, S.; Dünser, B.; Lezius, M.; Deutsch, H.; Becker, K.; Stamatovic, A.; Scheier, P.; Märk, T. D. *J. Chem. Phys.* **1996**, *105*, 1880.

(24) Qayyum, A.; Schustereder, W.; Mair, C.; Hess, W.; Scheier, P.; Märk, T. D. *Physica Scripta* **2003**, *T103*, 29.

(25) Qayyum, A.; Schustereder, W.; Mair, C.; Tepnual, T.; Scheier, P.; Märk, T. D. *Radiat. Phys. Chem.* **2003**, *68*, 257.

(26) Qayyum, A. Thesis, University of Innsbruck, 2002.

(27) Stockbauer, R. *J. Chem. Phys.* **1973**, *58*, 3800.

(28) Grill, V.; Walder, G.; Scheier, P.; Kurdel, M.; Märk, T. D. *Int. J. Mass Spectrom., Ion Proc.* **1993**, *129*, 31.

(29) Z. Prášil, Forst, W. *J. Chem. Phys.* **1967**, *71*, 3166.

(30) Mair, C.; Fedor, J.; Lezius, M.; Scheier, P.; Probst, M.; Herman, Z.; Märk, T. D. *New J. Phys.* **2003**, *5*, 9.1.

(31) von Koch, H. *Ark. Fys.* **1964**, *28*, 559.

(32) Kimura, K.; Katsumata, S.; Achiba, Y.; Yamazaki, T.; Iwata, S. *Handbook of HeI Photoelectron Spectra of Fundamental Organic Molecules* Japan Scientific Society Press: Tokyo, 1981.

(33) Stockbauer, R.; Inghram, M. G. *J. Chem. Phys.* **1975**, *62*, 4862

(34) Branton, G. R.; Frost, D. C.; Makita, T.; McDowell, C. A.; Stenhouse, I. A. *Philos. Trans. R. Soc. London A* **1970**, *268*, 77.

(35) Vestal, L. In *Fundamental Processes in Radiation Chemistry*; Ausloos, P.. Ed.) Wiley: New York, 1968; p. 59.

(36) Lindholm, E. In *Ion−Molecule Reactions*, Franklin, J., L., Ed.; Plenum: New York, 1972, Vol. 2, p 457.

(37) Jašík, J.; Žabka, J.; Ipolyi, I.; Feketeová, L.; Märk, T. D.; Herman, Z., to be published.

(38) Lias, S.; Bartmess, J. E.; Liebmann, J. F.; Holmes, J. L.; Levin, R. D.; Mallard, W. C. *J. Phys. Chem.* **1988**, Ref. Data 17, Suppl. 1.

(39) http://webbook.nist.gov/chemistry.